Springer

KSME

Journal of Mechanical Science and Technology 33 (9) (2019) 4255~4264
www.springerlink.com/content/1738-494x(Print)/1976-3824(Online)
DOI 10.1007/s12206-019-0822-z

# Role of TiC and h-BN particles on morphological characterization and surface effects of Al 4032 hybrid composites using EDM process †

T. S. Senthilkumar[1,*] and R. Muralikannan[2]

[1]*Department of Mechanical Engineering, Sree Sowdambika College of Engineering, Tamil Nadu, India*
[2]*Department of Mechanical Engineering, Sethu Institute of Technology, Tamil Nadu, India*

(Manuscript Received April 11, 2019; Revised May 30, 2019; Accepted June 3, 2019)

**Abstract**

Aluminum based hybrid metal matrix composites (HMMCs) are utilized in myriad of applications owing to their attractive properties such as low weight to high strength ratio, enriched mechanical and thermal properties over other conventional materials. In this work, the consequence of TiC and h-BN particles on morphological characterization and surface effects of aluminium based HMMCs during electrical discharge machining (EDM) process is discussed. The HMMCs are fabricated by varying the wt. % of TiC and then EDM is done by examining the input parameters such as peak current (A), pulse on time (μs) and gap voltage (v) under $L_{27}$ orthogonal array method. The performance and surface effects of the machined surface are evaluated after completing the EDM process. The MRR appears to surge with the rise in the peak current and decays with increasing the wt. % of TiC particles. Although by amplifying the wt. % of TiC particles, the size of the craters and the voids is augmented on the machined surface. Furthermore, as the peak current upsurges, the microhardness of the machined samples are augmented.

*Keywords*: EDM; Gap voltage (v); HMMCs; MRR; Microhardness; Pulse on time (μs); Peak current (A); TiC

## 1. Introduction

There has been rapid development of aluminum based metal matrix composite materials which are being utilized in the automobile field [1]. Ceramic materials such as SiC, $B_4C$, graphite, $Si_3N_4$, $Al_2O_3$ etc., are consumed as reinforcement materials to increase the strength of the aluminium alloy. By adding more than one reinforcement material it was named as "hybrid metal matrix composite" (HMMC) material. Distended tribological properties of HMMCs can be increased by adding secondary reinforcement particles such as graphite, BN, $Al_2O_3$ [2]. Kumar et al. [3] determined that the hardness and tensile property of the composite material was greater with the augmentation of TiC particles. Conversely, composite material density was also enhanced than that of the matrix alloy because of the higher density of TiC particles. Harichandran and Selvakumar [4] examined that the ductility and impact property of the hybrid composites have been increased due to the soft nature of h-BN particles. Plentiful techniques are available for fabricating the metal matrix composites. Among those techniques, stir casting is relatively economical, easily fabricated and can be obtainable for bulk production [5].

The aluminum metal matrix composite acquired through stir casting route is applicable in the production of disc brakes, cylinder liners and drive shaft manufacturing sectors [6]. For such applications, conventional machining is not effectivel due to the addition of hard ceramic particles in the matrix. So, the unconventional machining process was desired for machining the metal matrix composite material [7]. There are many types of unconventional machining process, such as electrical discharge machining (EDM), wire electrical discharge machining (WEDM), electro chemical machining (ECM), electron beam machining (EBM), ultrasonic machining (USM) and abrasive water jet machining (AWJM). Among the numerous unconventional machining, the electrical discharge machining (EDM) process is the desired technique for machining particle reinforced metal matrix composites [8]. There are numerous parameters in EDM to obtain the improved machining characteristics. The main machining performance of the EDM process consists of metal removal rate (MRR), tool wear rate (TWR), surface roughness (SR), and over cut (OC).

Achieving more metal removal rate (MRR), greater surface finish with a lesser amount of power consumption is the foremost expectation of today's industry. Moreover, the electrode wear ratio has to be minimized to increase

*Corresponding author. Tel.: +91 99524 60423, Fax.: +91 4566 228232
E-mail address: senthilk.kumar6@gmail.com
† Recommended by Associate Editor Tae June Kang

productivity. Muthuramalingam et al. [9] investigated that the electrical conductivity of the electrode material plays a vital role over the machined surface. Czelusniak et al. [10] reveal that materials which have high electrical conductivity and high thermal conductivity could be used as EDM electrodes. The surface quality of the machined surface using graphite electrodes was found to be lesser when compared with copper electrodes [11].

Uthayakumar et al. [12] exposed that the minor pulse on time and pulse current created enhanced result. Ahmed et al. [13] stated that for high metal removal rate in $B_4C$ and SiC reinforced materials, extended duration of spark was necessary with a large value of flushing pressure. Kumar et al. [14] represented that the escalation of peak current and pulse on time stimulates greater crater size, which provides poor surface finish. Kumar and Prakash [15] studied the experimental investigation and optimization of EDM process parameters for machining (Al-$B_4C$) composite, and from this study they signified that the metal removal rate increases with surging up the current and EWR also amplified linearly with intensification of peak current. Islam Shyha and Rudd [16] determined that by increasing discharge current, a high removal rate with high tool wear rate was accomplished. Gopalakannan and Senthilvelan [17] determined that the surface roughness augments with upsurge in both the peak current and pulse on time and also that the electrode wear rate declines with enriching the pulse off time. Senthilkumar and Omprakash [18] showed that the MRR of composite material was increased with elevation in discharge current, while it was diminished with ris in wt. % of titanium carbide particles in the composite material.

Mahanta [19] reported that a coarser surface was produced with larger crater at high input energy. Rajesha et al. [20] held that at the process parameter condition of peak current 15 Amps, pulse on-time 10 µs and pulse off-time 6 µs, however, surface roughness was found. Singh et al. [21] examined the cross-sectional microhardness of the machined surface gradually decreased along the depth of the surface. Garg et al. [22] deliberated about the research work sinking EDM and WEDM on metal matrix composite materials. From this discussion they described that maximum of work was carried on SiC reinforced metal matrix composites.

From the above reviews it seems that there are a few EDM research works that have been achieved in the hybrid metal matrix composite (HMMC) materials. Although, there are no EDM works on machining of TiC and h-BN reinforced HMMCs material. In this work, the ceramic materials namely TiC with different wt. % (3wt. % and 6wt. %) and h-BN with constant wt. % (2wt. %) were reinforced with aluminium alloy 4032. The hybrid metal matrix composite materials were fabricated by exploiting stir casting routine. Further, the EDM process was carried out on the fabricated composite materials. Hence, for executing the machining the three input parameters, namely pulse on time, peak current and gap voltage, were nominated and these parameters were organized on the basis of $L_{27}$ orthogonal array. The machining was finished on all the three samples of hybrid metal matrix composite materials. The influence of process parameters and addition of TiC-h-BN particles were analyzed on the machinability properties like metal removal rate, tool wear rate and surface roughness. Moreover, surface integrity elements such as microstructure of machined surface and microhardness were also investigated.

Table 1. Prepared wt. % of hybrid metal matrix composite materials.

| S. No. | Al alloy 4032 (wt. %) | Titanium carbide (wt. %) | h-boron nitride (wt. %) |
|---|---|---|---|
| Sample I | 100 | 0 | 0 |
| Sample II | 95 | 3 | 2 |
| Sample III | 92 | 6 | 2 |

## 2. Experimental work

### *2.1 Materials and fabrication process*

The aluminum-silicon alloy (Al 4032) is nominated as the matrix material and TiC (Titanium Carbide) and h-BN (hexagonal - Boron Nitride) are designated as the reinforcement materials, procured from Sigma Aldrich, Germany. Totally, three samples were prepared by varying the wt. % of TiC and h-BN particulates which has been denoted in Table 1.

Stir casting manner is considered for the fabrication of hybrid composite materials. The procedure for making the hybrid composite materials is discussed below.

A pure aluminium alloy 4032 was produced without adding the reinforcement particles. The remaining two samples were prepared by adding the reinforcement particulates. The preparation method of HMMCs is explained below. Stir casting is considered for the fabrication of hybrid composite materials. The matrix material was preheated on a furnace at 400 ºC. Correspondingly, the prepared reinforcement materials were also preheated to 1000 ºC. Once again, the preheated aluminium alloy was heated beyond its melting point to attain the liquid state. To dismiss the impurities present in the molten metal, degasser powder was added. Moreover, the coverall powder was added in to the liquified metal to maintain the temperature inside of the crucible. Subsequently, the preheated reinforcement materials were manually added into the molten metal and mixed mechanically with the support of mechanical stirrer up to 10 minutes at a speed of 500 RPM to disseminate the reinforcement materials homogeneously into the matrix material.

After mixing the melt, the temperature was maintained up to 750 ºC for superior bonding between the matrix and reinforcement. Further, the mixed liquid was poured into the preheated die having dimensions of 100 mm x 100 mm x 10 mm. This fabrication process was repeated for the remaining sample. Thereafter, the pure Al alloy 4032 and fabricated composite materials were led for machining in electrical discharge machine (EDM).

Table 2. Parameters and their levels.

| Parameters | Unit | Levels | | |
|---|---|---|---|---|
| | | 1 | 2 | 3 |
| Peak current (I) | A | 9 | 12 | 15 |
| Pulse on time ($T_{on}$) | µs | 50 | 75 | 100 |
| Gap voltage (V) | v | 30 | 35 | 40 |

### *2.2 Experimental setup and methodology*

The machining of hybrid composite materials is carried on a die sinking electrical discharge machine. A copper rod with 10mm diameter and 80 mm height was utilized as electrode. In this experiment kerosene with a viscosity of 2.71cs at 200 C and a flushing pressure of 1.3 kg/cm$^2$ was engaged as a dielectric medium to avoid erosion between the workpiece and electrode.

The positive terminal was connected to the workpiece material and placed on the machine bed, and the negative terminal was connected to the copper electrode. The workpiece and the electrode were immersed in the closed machined bed until it was submerged in the dielectric medium.

The parameters and its levels of EDM process used in the EDM process are mentioned in Table 2. The experiments were conducted using experimental design namely $L_{27}$ orthogonal array as shown in Table 3. A blind hole with a depth of 2 mm and diameter of 10 mm was produced on the workpiece surface. Thus, the machining was done for all the experiments.

The metal removal rate (MRR) values were determined by calculating the weight loss of the composite material previously and afterward the machining irrespective to the machining time. Tool wear rate (TWR) was calculated by calculating the weight loss of the electrode tool before and after the machining irrespective of the time elapsed for machining. A high precision weighing balance having an accuracy of ±0.1 mg was utilized to calculate the weight loss. The surface roughness values were measured by Mitutoyo SJ 410 with probe speed of 0.5 mm/s and a transverse length of 5 mm. The performance measurements were calculated for all the samples. The microstructure of the machined samples was investigated using scanning electron microscopy (SEM). The microhardness of the machined sample (cross-section) was envisioned using Vickers microhardness tester.

## 3. Results and discussion

### *3.1 Microstructure of composite materials*

The produced composite materials underwent a microstructure analysis by SEM image.

Fig. 1(a) demonstrates SEM with EDS mapping of Al alloy 4032. From the figure, the chemical composition such as Si, Mg, Ni and Cu was also achieved. Also, for the composite materials the SEM with EDS mapping was undergone, and the results are in Figs. 1(d) and (g). The figure confirms that the reinforcement particles have been uniformly scattered in the matrix material after stir casting route. It has been recognized as a consistent EDS analysis.

Table 3. Experimental design.

| S. No. | Current (A) | Pulse on time (µs) | Gap voltage (V) |
|---|---|---|---|
| 1 | 9 | 50 | 30 |
| 2 | 9 | 50 | 35 |
| 3 | 9 | 50 | 40 |
| 4 | 9 | 75 | 30 |
| 5 | 9 | 75 | 35 |
| 6 | 9 | 75 | 40 |
| 7 | 9 | 100 | 30 |
| 8 | 9 | 100 | 35 |
| 9 | 9 | 100 | 40 |
| 10 | 12 | 50 | 30 |
| 11 | 12 | 50 | 35 |
| 12 | 12 | 50 | 40 |
| 13 | 12 | 75 | 30 |
| 14 | 12 | 75 | 35 |
| 15 | 12 | 75 | 40 |
| 16 | 12 | 100 | 30 |
| 17 | 12 | 100 | 35 |
| 18 | 12 | 100 | 40 |
| 19 | 15 | 50 | 30 |
| 20 | 15 | 50 | 35 |
| 21 | 15 | 50 | 40 |
| 22 | 15 | 75 | 30 |
| 23 | 15 | 75 | 35 |
| 24 | 15 | 75 | 40 |
| 25 | 15 | 100 | 30 |
| 26 | 15 | 100 | 35 |
| 27 | 15 | 100 | 40 |

The elemental mapping of Al alloy 4032 is shown in Fig. 1(b). Elements such as Al and Si particles can be seen. Additionally, the composition of base metal Al 4032 likely Mg, Ni and Cu were also present in little amount. The EDS analysis of the mapping is indicated in Fig. 1(c), as it implied that the peak represents the deviation of the chemical composition of Al alloy 4032.

Fig. 1(e) and h describe the elemental mapping of Al4032-3 %TiC-2 % h-BN and Al4032-6 %TiC-2 % h-BN composite material, respectively. Figures asserted that B, N, Ti and C have been effectively combined by the stir casting process in the matrix (Al 4032). In a similar work the elements were present as shown in the images [23]. Figs. 1(f) and (i) display the EDS analysis of the elemental mapping of composite materials; it implies that high intensity, medium intensity and low intensity peaks represent the deviation of the secondary particles, respectively.

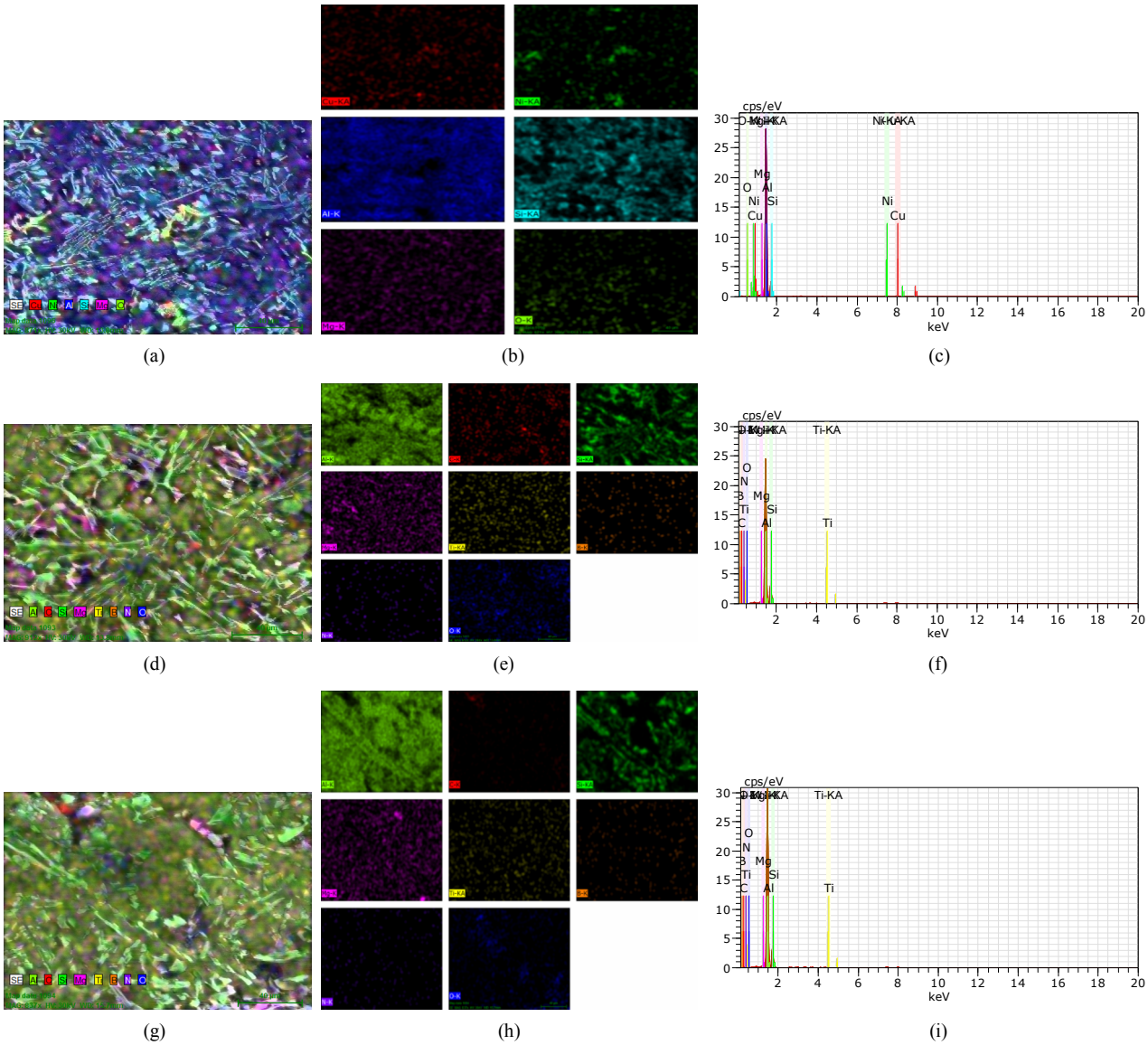


Fig. 1. SEM with EDS mapping of (a) Al alloy 4032; (d) Al4032-3%TiC-2% h-BN composite material; (g) Al4032-6%TiC-2% h-BN composite material and elemental mapping of (b) Al alloy 4032; (e) Al4032-3%TiC-2% h-BN composite material; (h) Al4032-6%TiC-2% h-BN composite material and EDS analysis of the elemental mapping of (c). Al alloy 4032; (f) Al4032-3%TiC-2% h-BN composite material; (i) Al4032-6%TiC-2% h-BN composite material.

The appearance of various colors such as green, red, violet and purple, respectively, indicates the occurrence of all elements which map overlay. It is also determined that those elements are not combinations with any of the others in some areas.

### *3.2 Influence of process parameters and addition of TiC-h-BN on MRR*

Figs. 2(a)-(c) illustrates the effect of metal removal rate under the parameters such as peak current, pulse on time and gap voltage for Al alloy 4032 and composite materials such as Al4032-3 %TiC-2 % h-BN and Al4032-6 %TiC-2 % h-BN. Results demonstrate that the MRR enhances with increasing the input process parameters.

Fig. 2(a) defines the effects of MRR under the condition of peak current for Al 4032 alloy and TiC-h-BN reinforced composites. From the figure it clearly represents that the MRR was augmented with improving the peak current. Nevertheless, the MRR was truncated for the composite materials when related to the pure Al alloy 4032 due to the occurrence of hard particles, namely TiC which has a shielding effect.

Fig. 2(b) reveals that the MRR augments while proliferation of the pulse on time because the discharge energy gets increased at high pulse on time, which surges the elimination of more material. But the MRR is condensed for the composite materials such as Al4032-3 %TiC-2 % h-BN and Al4032-6 %TiC-2 % h-BN.

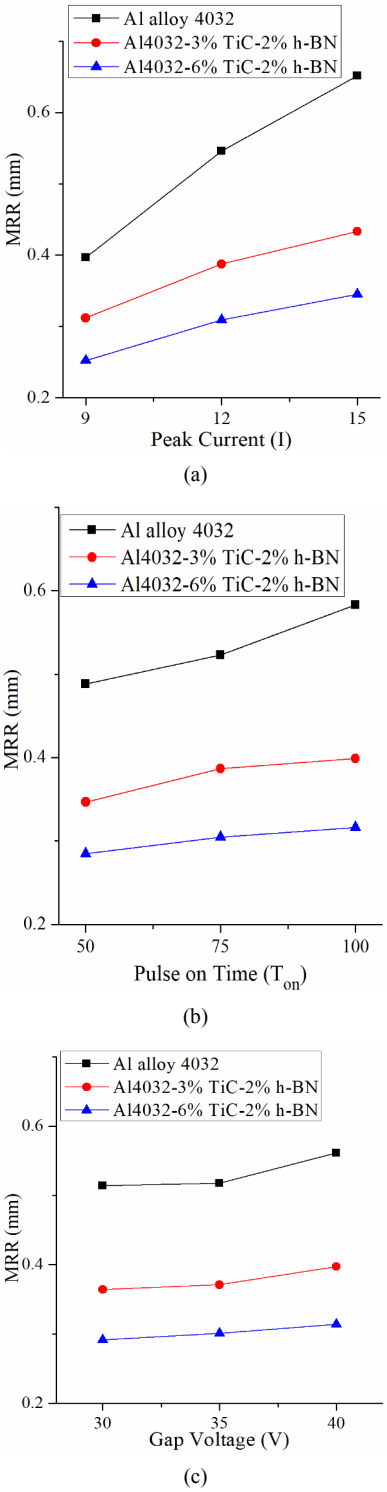


Fig. 2. (a) Effects of MRR under peak current (A); (b) effects of MRR under pulse on time (μs); (c) effects of MRR under gap voltage (v).

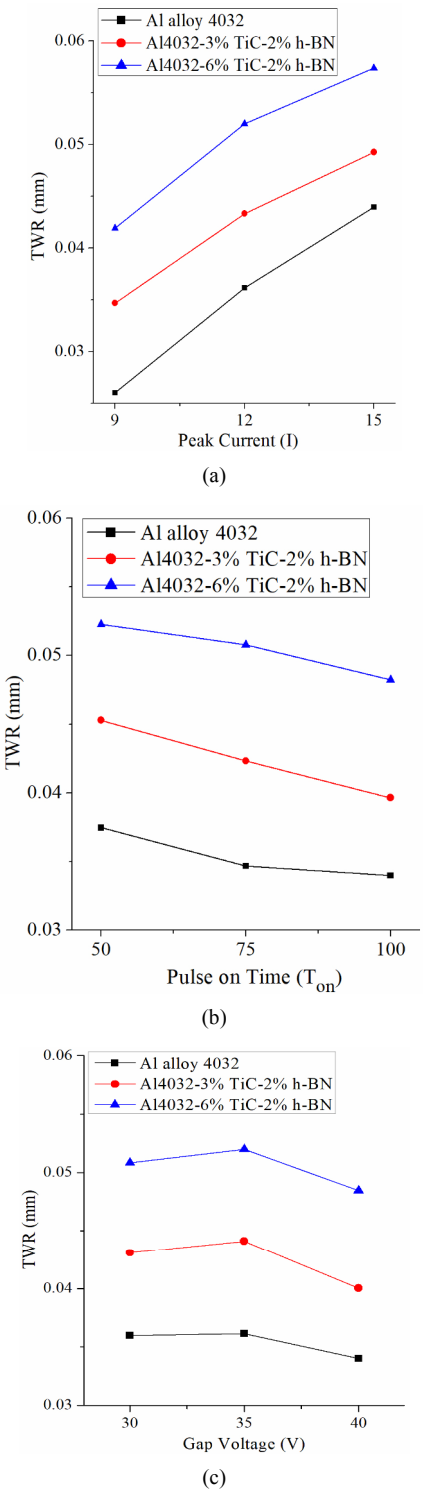


Fig. 3. (a) Effects of TWR under peak current (A); (b) effects of TWR under pulse on time (μs); (c) effects of TWR under gap voltage (v).

Because the TiC particles have a huge amount of density, they won't get cleaned away by dielectric medium, as some amount of the TiC particles will get stuck in the matrix material and form a new layer known as recast layer, and thus the elimination of the material gets reduced. This result can be summarized by augmenting the flushing pressure of the dielectric medium.

The MRR slightly develops by enhancing the gap voltage as shown in Fig. 2(c). The figure clarifies that as the gap voltage increases, the MRR also improves throughout the results.

With rise in spark gap, the energy is spread uniformly, which results in upsurge the sparking frequency and pressure within the plasma channel, thereby MRR is improved.

The reason for less MRR for TiC-h-BN reinforced composites is because of tremendous thermal resistance of titanium carbide particles, and thermal spalling transpired during the machining process. As the peak current upsurges, the produced discharge energy augments thermal spalling. Therefore, the MRR of composite materials could increase with peak current.

Furthermore, the MRR is reduced in the hybrid metal matrix composite materials due to the occurrence of h-BN particles. The h-BN particles have good bonding properties which have well bonded in the matrix material and thus the MRR was reduced.

### *3.3 Influence of process parameters and addition of TiC-h-BN on TWR*

Figs. 3(a)-(c) relate the influence of process parameters, namely peak current (A), pulse on time (μs) and gap voltage (v) on TWR.

The effect of TWR under the circumstance of peak current is shown in Fig. 3(a). It clearly shows that the TWR increases throughout the value of peak current because of high thermal effect. As the current increases, more thermal energy is produced in the spark gap, which leads to the formation of electrode erosion and therefore it results in increased TWR. Nonetheless, the TWR is low for the Al alloy 4032 when related to the TiC reinforced content composite materials because the TiC particles get trapped in the spark gap to enable more intensity of plasma arc and decrease the dielectric fluid pressure to continue the machining process.

The TWR rate decreased with improving the pulse on time for the three materials, as demonstrated in Fig. 3(b). This result may due to extension in pulse on time that increases the extraordinary discharge energy, which allows the removal of excess material from the workpiece. Thus, the prolonged pulse on time develops a machining cavity and craters are produced on the surface. The TWR performance has a temperate range while evolution in pulse on time. Similar results have been attained for TWR under pulse on time [24].

The tool wear rate was affected by gap voltage as it was demonstrated in Fig. 3(c). It demonstrates that the TWR moderately amplified with intensifying the gap voltage up to 35 V, because less material is removed from the workpiece. Further escalating the gap voltage beyond 35 V, the TWR decreased. This is attributed to that after high gap voltage creates a prolonged spark energy which increases the MRR and reduces the TWR.

Nevertheless, on machining the Al alloy 4032 and TiC-h-BN reinforced composite materials with different wt. %, the TWR enlarges with increasing the wt. % of TiC particles. This result is attributed to that the TiC particles are abrasive in nature [18].

Moreover, the TWR range declines more in the TiC-h-BN reinforced composites when related to the Al alloy 4032. This phenomenon is due to the solid lubricant properties of h-BN particles which provide erosion of tool electrode.

### *3.4 Influence of process parameters and addition of TiC-h-BN on SR*

The SR of Al alloy 4032 and TiC-h-BN reinforced composite materials under the conditions of process parameters peak current (A), pulse on time (μs) and gap voltage (v) respectively is shown in Figs. 4(a)-(c). As the peak current increases the discharge energy increases, which permits the development of aggressive forces on the workpiece surface, and a poor surface is achieved. Hence, the SR improves with augmenting the peak current throughout its range as shown in Fig. 4(a).

The SR value increases continuously with increase in pulse on time as in Fig. 4(b). Due to the increment of pulse on time, huge volume of spark energy is produced between the workpiece and tool electrode. Therefore, more cracks are possible to overlap on the machined surface. As the pulse on time rises, the period of discharge energy increases, which permits the elimination of excess material from the work piece surface and intensification in SR. Furthermore, the machined surface is affected by deeper and huge discharge craters by amplifying the peak current and pulse on time [25].

Fig. 4(c) also shows that SR is increased owing to the growth in gap voltage. Furthermore, the SR is enhanced with amplifying the wt. % of TiC because of its high heat resistance. This result occurs because a trivial amount of TiC particles that get trapped on the machined surface affect the surface finish and a coarser surface results.

Furthermore, the range of SR decays for TiC-h-BN reinforced composite materials at three input parameter conditions because of self-lubricating properties of h-BN particles, which forms a thin protective layer on the machined surface.

### *3.5 Microstructural analysis of machined surface*

The machined surfaces of the Al alloy 4032 and TiC-h-BN reinforced composite materials were observed using SEM as shown in Figs. 5(a)-(c). Fig. 5(a) illustrates the microstructure of EDM machined surface of the Al alloy 4032 at I = 15A; $T_{on}$ = 100 μs; V = 40 V. A smaller number of voids are present in surface due to high peak current and pulse on time. The crater is attained owing to the realization of bombarding force during excessive peak current [14]. Hence, small number of voids and crater were produced. The extent of the crater and voids can be summarized or may be avoided under the circumstance of low peak current because less discharge energy was created, and little material was detached. However, the surface is uniform and smooth as illustrated in Fig. 5(a).

The machined surface of Al4032-3 % TiC-2 % h-BN composite material is displayed in Fig. 5(b). Fig. 5(b) shows that the extent of the crater and the voids on the machined surface

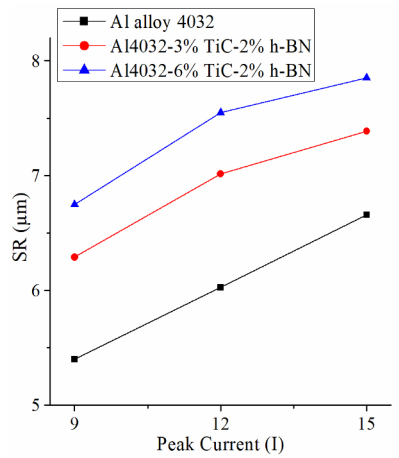


(a)

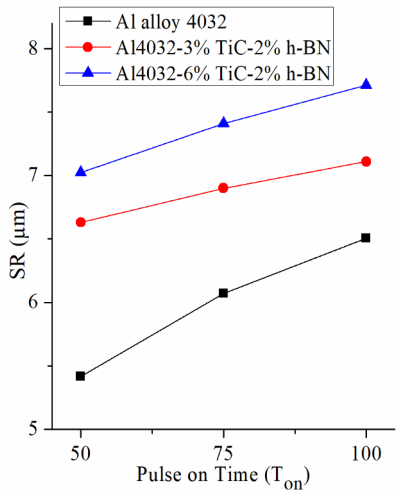


(b)

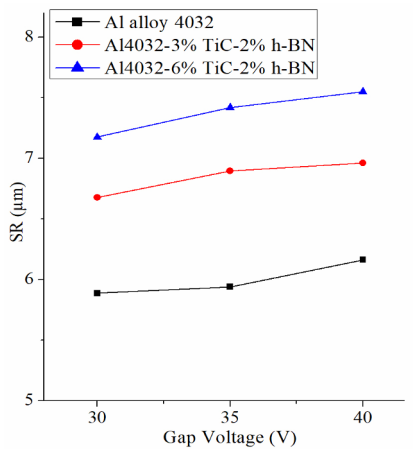


(c)

Fig. 4. (a) Effects of SR under peak current (A); (b) effects of SR under pulse on time (µs); (c) effects of SR under gap voltage (v).

of TiC reinforced composite material is high when correlated to the machined surface of Al alloy. This result is achieved because of the occurrence of hard reinforcement particles such as TiC. The TiC particle will not get solidified for the reason

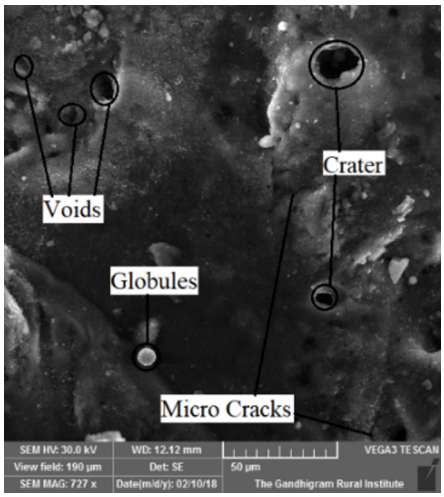


(a)

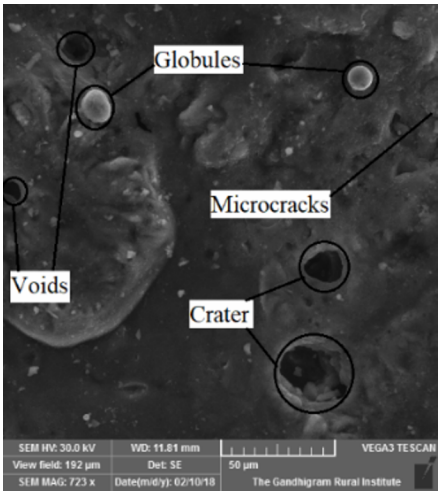


(b)

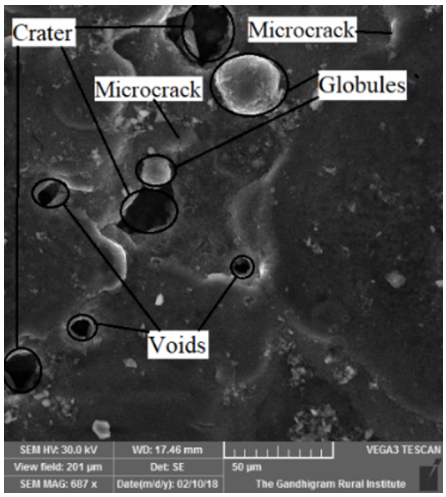


(c)

Fig. 5. (a) Microstructure of machined surface at I = 15A; $T_{on}$ = 100 µs; V = 40v for Al alloy 4032; (b) microstructure of machined surface at I = 15 A; $T_{on}$ = 100 µs; V = 40v for Al4032-3 %TiC-2 % h-BN; (c) microstructure of machined surface at I = 15A; $T_{on}$ = 100 µs; V = 40v for Al4032-6 %TiC-2 % h-BN.

of its high melting point, as it is flushed away by the dielectric medium with high pressure. During the timing of flushing some of the TiC particles get removed from the matrix material, which leads to the enlargement of the crater size.

Also, globules were seen on the machined surface. This may be documented by the incidence of tremendous thermal resistance of the TiC particles. Also, the wettability property of TiC particles affects the matrix material [26]. Hence, the MRR is reduced owing to the heat resistance of TiC particles.

Moreover, metallurgical transformation was accomplished on the machined surface due to the establishment of high temperature at high peak current and high pulse on time, which results as microcracks owed to the internal stresses.

The microstructure of machined surface of Al4032-6 %TiC-2 % h-BN composite material is exhibited in Fig. 5(c). It shows that more craters, voids and micro cracks were present when compared to the Al4032-3 %TiC-2 % h-BN composite material because of increment in addition of TiC particles, as the wt. % of TiC particles upsurges, the quantity of the crater increases. Moreover, more discharge energy is produced at prolonged time, which allows the upsurge of size of crater and formation of poor surface [27]. Anyhow, the extent of the crater was somewhat reduced due to the appearance of h-BN particles in the composite materials.

At high gap voltage, a higher impulsive force was formed, which was responsible for poor surface finish as represented in Fig. 5(c). Furthermore, at high peak current more thermal energy formed which created a blasting force in the workpiece surface, resulting as increase in a greater number of voids as seen in Fig. 5(c). Similar results was obtained for increased peak current on the machined surface [12].

Besides, due to high peak current and high pulse on time, the stress occurring on the machined surface exceeds the ultimate stress of the composite materials, which leads to the development of microcracks. Moreover, the microcracks were amplified while augmenting the wt. % of TiC particles. Nevertheless, the enlargement of the microcracks is reduced with addition of h-BN particles, which emphasizes the thermal shock resistance.

### *3.6 Microhardness of machined surface*

In order to measure the microhardness, the ED machined cross-sectional composite samples were prepared by water jet machining (WJM) process. Afterward, the microhardness was measured on the polished ED machined samples using Vickers micro hardness tester at cross-section by applying 100 g load for a time of 10 s. The microhardness value is determined along depth from the machined surface. Results of microhardness of the machined samples under the circumstance of peak current = 15 A; pulse on time = 100 µs and gap voltage = 40 v are shown in Fig. 6.

Fig. 6 clarifies that the microhardness of the machined Al4032-6 %TiC-2 % h-BN sample is higher when related to the remaining two samples because of greater content of TiC particles in the matrix material [28]. Although, the microhardness of the recast layer and at the heat affected zone (HAZ) is high for the TiC-h-BN reinforced composite materials when equated to the matrix material Al alloy 4032 due to the appearance of TiC particles on the recast layer surface. Besides, the microhardness diminishes along the depth from the machined surface, i.e., heat affected zone when linked to the recast layer area because the HAZ has moderating effect due to the thermal degradation in the discharging process. The reason for reduction in hardness of HAZ is due to the occurrence of h-BN particles which have soft property.

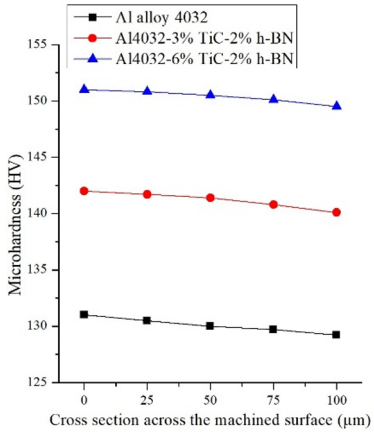


Fig. 6. Microhardness of machined surface.

The microhardness range obtained for all the samples is the same. The microhardness increased due to the deposition of copper material on the recast layer which was eroded from the electrode during the machining time. Moreover, the copper material has high melting temperature, which has a rapid temperature change (i.e., rapid cooling), and thus the hardness was augmented. This was due to the ageing effect [29]. The copper material dumped on all the machined samples was already mentioned in the EDS analysis. Besides, the microhardness of the machined samples augmented as the peak current increased due to the formation of pulsation energy. Likewise, the microhardness was reduced with increasing the pulse on time because more discharge energy was produced, which creates more heat and thus stress occurred on the machined surface.

## 4. Conclusions

The aluminum alloy 4032 was successfully fabricated through the stir casting method with varying wt. % (3 wt. % & 6 wt. %) of TiC particles and constant wt. % (2 wt. %) of h-BN particles. Then the fabricated samples were machined through electrical discharge machining (EDM) process and the subsequent conclusions were attained:

- The MRR augmented with increased pulse on time. However, the MRR diminished by enhancing the wt. % of TiC particles due to its low thermal conductivity.
- SR was enlarged with increased peak current and pulse on time. However, the SR range was reduced for TiC-h-

BN reinforced composite materials when compared to Al alloy 4032.

- At high peak current and high pulse on time, microcracks developed on the machined surfaces. Besides, the size of the crater and the voids on the machined surface enlarged with increasing the wt. % of TiC.
- The microhardness of the recast layer is high for Al4032-3 %TiC-2 % h-BN composite material with a value of 151HV due to the deposition of copper material eroded from electrode.

## References


[1] K. K. Chawla and N. Chawla, Metal matrix composites: Automotive applications, *Encyclopedia of Automotive Engineering* (2014) 1-6.

[2] S. T. Kumaran and M. Uthayakumar, Investigation on the dry sliding friction and wear behavior of AA6351-SiC-B4C hybrid metal matrix composites, *J. of Engineering Tribology,* 228 (3) (2014) 332-338.

[3] K. R. Kumar, K. Kiran and V. S. Sreebalaji, Micro structural characteristics and mechanical behaviour of aluminium matrix composites reinforced with titanium carbide, *J. of Alloys and Compounds,* 723 (2017) 795-801.

[4] R. Harichandran and N. Selvakumar, Microstructure and mechanical characterization of ($B_4C$+ h-BN)/Al hybrid nanocomposites processed by ultrasound assisted casting, *International J. of Mechanical Sciences,* 144 (2017) 814-826.

[5] M. T. Alam et al., Mechanical properties and morphology of aluminium metal matrix nanocomposites-stir cast products, *Advances in Materials and Processing Technologies,* 3 (4) (2017) 600-615.

[6] A. R. Ahamed et al., Drilling of hybrid Al-5%SiCp-5%$B_4Cp$ metal matrix composites, *International J. of Advanced Manufacturing Technology,* 49 (9-12) (2010).

[7] A. Pramanik, Developments in the non-traditional machining of particle reinforced metal matrix composites, *International J. of Machine Tools and Manufacture,* 86 (2014) 44-61.

[8] K. H. Ho and S. T. Newman, State of the art electrical discharge machining (EDM), *International J. of Machine Tools and Manufacture,* 43 (13) (2003) 1287-1300.

[9] T. Muthuramalingam, B. Mohan and S. Vignesh, Performance analysis of pulse generators on residual stress of machined silicon steel using the EDM process, *Silicon,* 10 (5) (2018) 1785-1792.

[10] T. Czelusniak et al., Materials used for sinking EDM electrodes: A review, *J. of the Brazilian Society of Mechanical Sciences and Engineering,* 41 (1) (2019) 14.

[11] V. J. Mathai, H. K. Dave and K. P. Desai, Experimental investigations on EDM of Ti6Al4V with planetary tool actuation, *J. of the Brazilian Society of Mechanical Sciences and Engineering,* 39 (9) (2017) 3467-3490.

[12] M. Uthayakumar, K. Vinoth Babu, S. Thirumalai Kumaran, S. Suresh Kumar, J. T. Winowlin Jappes and T. P. D. Rajan, Study on the machining of Al-SiC functionally graded metal matrix composite using die-sinking EDM, *Particulate Science and Technology,* 37 (1) (2017) 103-109.

[13] A. R. Ahamed, P. Asokan and S. Aravindan, EDM of hybrid Al-SiCp-$B_4Cp$ and Al-SiCp-Glassp MMCs, *The International J. of Advanced Manufacturing Technology,* 44 (5-6) (2009) 520-528.

[14] S. S. Kumar, M. Uthayakumar, S. Thirumalai Kumaran and P. Parameswaran, Electrical discharge machining of Al(6351)-SiC-$B_4C$ hybrid composite, *Materials and Manufacturing Processes,* 29 (11-12) (2014) 1395-1400.

[15] P. Kumar and R. Parkash, Experimental investigation and optimization of EDM process parameters for machining of aluminum boron carbide (Al-$B_4C$) composite, *Machining Science and Technology,* 20 (2) (2016) 330-348.

[16] I. Shyha and M. Rudd, Electro-discharge machining of metal matrix composite materials, *Advances in Materials and Processing Technologies,* 2 (2) (2016) 235-244.

[17] S. Gopalakannan and T. Senthilvelan, A parametric study of electrical discharge machining process parameters on machining of cast Al/B4C metal matrix nanocomposites, *Proceedings of the Institution of Mechanical Engineers, Part B : J. of Engineering Manufacture,* 227 (7) (2013) 993-1004.

[18] V. Senthilkumar and B. U. Omprakash, Effect of titanium carbide particle addition in the aluminium composite on EDM process parameters, *J. of Manufacturing Processes,* 13 (1) (2011) 60-66.

[19] S. Mahanta, M. Chandrasekaran, S. Samanta and R. M. Arunachalam, EDM investigation of Al 7075 alloy reinforced with B4C and fly ash nanoparticles and parametric optimization for sustainable production, *J. of the Brazilian Society of Mechanical Sciences and Engineering,* 8 (40) (2018) 263.

[20] Rajesha S., C. S. Jawalkar, R. Raman Mishra, A. K. Sharma and P. Kumar, Study of recast layers and surface roughness on Al-7075 metal matrix composite during EDM machining, *International J. of Recent Advances in Mechanical Engineering,* 3 (1) (2014) 53-62.

[21] B. Singh, J. Kumar and S. Kumar, Experimental investigation on surface characteristics in powder-mixed electrodischarge machining of AA6061/10%SiC composite, *Materials and Manufacturing Processes,* 29 (3) (2014) 287-297.

[22] R. K. Garg, K. K. Singh, A. Sachdeva, V. S. Sharma, K. Ojha and S. Singh, Review of research work in sinking EDM and WEDM on metal matrix composite materials, *The International J. of Advanced Manufacturing Technology,* 50 (5-8) (2010) 611-624.

[23] S. Aksoz, A. T. Ozdemir, R. Calin, Z. Altonik and B. Bostan, Effects of sintering, ageing and cryogenic treatments on structural and mechanical properties of AA2014-B4C composite, *J. of the Faculty of Engineering and Architecture of Gazi University*, 28 (4) (2013) 831-839.

[24] B. Singh, J. Kumar and S. Kumar, Investigation of the tool wear rate in tungsten powder-mixed electric discharge machining of AA6061/10%SiCp composite, *Materials and Manufacturing Processes,* 31 (4) (2016) 456-466.

[25] M. Hourmand, S. Farahany, A. A. D. Sarhan and M. Yusof

Noordin, Investigating the electrical discharge machining (EDM) parameter effects on Al-$Mg_2Si$ metal matrix composite (MMC) for high material removal rate (MRR) and less EWR-RSM approach, *International J. of Advanced Manufacturing Technology,* 77 (5-8) (2015) 831-838.

[26] S. Aksöz and B. Bostan, Effects of the AA2014/B4 C MMCs production with casting and post casting sintering operations on wear behaviors, *Journal of Boron,* 3 (2) (2018) 132-137.

[27] T. S. Senthilkumar and R. Muralikannan, Enhancing the geometric tolerance of aluminium hybrid metal matrix composite using EDM process, *J. of the Brazilian Society of Mechanical Sciences and Engineering,* 41 (1) (2019) 41.

[28] E. Tan, Y. Kaplan, H. Ada and S. Aksöz, *Production of the AA2196-TiB2 MMCs via PM Technology*, Chesonis C. (eds), Light Metals. The Minerals, Metals & Materials Series, Springer, Cham. (2019) 153-157.

[29] A. Taskesen, S. Aksöz and A. T. Özdemir, The effect of cryogenic treatment on ageing behaviour of $B_4C$ reinforced 7075 aluminium composites, *Metallic Materials,* 55 (1) (2017) 57-67.

**T. S. Senthilkumar** is an Assistant Professor of Mechanical Engineering at Sree Sowdambika College Engineering, Aruppukottai, India. He completed his B.Tech. in Mechanical Engineering at Kalasalingam University, Krishnakoil Tamilnadu, India and M.E. in Engineering Design at Paavai Engineering college, Namakkal, Tamilnadu, India.

**R. Muralikannan** is a Professor in the Mechanical Engineering at Sethu Institute of Technology, Kariapatti, Tamil Nadu, India. His B.E. in Mechanical Engineering is from PSNA College of Engineering and Technology, Dindigul, Tamilnadu, India. His M.E. in CAD/CAM is from Mepco Schlenk Engineering College, Sivakasi, India and his Ph.D. is from IIT madras, Tamilnadu, India.